POLITECNICO
MILANO 1863

SCUOLA DI INGEGNERIA INDUSTRIALE
E DELL'INFORMAZIONE

Executive Summary of the Thesis

Study of an auxetic cardiac patch capable of conducting electrical signals while minimizing the impact on the mechanical functionality of an infarcted ventricle

Master of Science in Biomedical Engineering and Mechanical Engineering

Authors: Nisida Masullo, Veronica Luppini

Advisors: Prof. Jose Felix Rodriguez Matas, Prof. Stefano Foletti

Co-advisors: Ing. Francesca Berti, Ing. Ludovica Cestariolo, Ing. Matteo Gavazzoni

Academic year: 2022-2023

1. Introduction

In Italy, approximately 45% of mortality is attributed to cardiovascular diseases, and among these, ischemic heart disease accounts for about 35% of deceases [10]. Myocardial ischemia arises from insufficient oxygen supply, causing cell damage. A prolonged oxygen deficiency impacts on both ventricular mechanics and myocardial cell electrical properties. At present, no curative devices are available to treat myocardial infarction, except for a limited number of approaches focused on repairing damaged cardiac or vascular tissue without establishing electrical integration with the tissue. A promising area of research involves myocardial tissue engineering, using hydrogels, scaffolds, and patches to support damaged tissue through cellular and non-cellular approaches. For the latter, it's crucial to restore the electrical properties while maintaining normal heart function. As a result, the mechanical properties of the patch should closely match those of heart tissue. This thesis aimed to explore the feasibility of utilizing an optimization tool to obtain the desired mechanical properties in an auxetic patch. Mechanical simulations were carried out to assess how the patch affected ventricle deformation throughout the cardiac cycle. Then, an electrophysiological study was conducted to evaluate the patch conductivity, specifically its ability to transmit the electrical signals of myocardial cells.

2. Patch geometry definition

An adequate patch must have mechanical and electrical properties as similar as possible to those of the healthy myocardial tissue [8]. Since the overall behavior of the ventricular musculature is auxetic [2, 3], the patch must be formed by a series of repeated unit cells whose macroscopic response is auxetic as well.
For the definition of patch geometry, a topology optimization tool was used [7]. This tool solves an inverse homogenization problem by density-based topology optimization at the microscale, guided by requirements on the macroscopic mechanical and conductive properties of the unitary cell. Hence, the inputs to the tool are the bulk material properties (Young's modulus, Poisson's ratio, electrical conductivity) and the patch requirements. The output is a unitary cell structure, supplied in *.vtk* format, with a specific density distribution which satisfies the boundary conditions imposed.
The code allows to control the components of the stiffness matrix and the elements of the conductivity matrix. The former are function of the Young's modulus and Poisson's ratio. The latter were imposed in accordance to values directly sourced from literature. The desired mechanical and conductive properties are the ones of the heart tissue: $E_1 = 0.1 \div 0.5\ MPa$ is the transverse stiffness, indicating the circumferential direction of the heart fibers, $\frac{E_2}{E_1} = 0.25 \div 0.5$ is the stiffness ratio, being E_2 the longitudinal stiffness, $\nu =$

$-0.8 \div -0.2$ is the Poisson's ratio, $k_1 = 0.2 \div 0.8\, S/m$ is the transverse conductivity, and $\frac{k_2}{k_1} = 0.3 \div 0.8$ is the conductivity ratio, being k_2 the longitudinal conductivity.

The optimization tool is based on mass minimization, that is not an objective function tailored for this application. Nevertheless, it allows to obtain a structure that is physically reasonable. One of the purposes of topology definition is to get a robust and easily manufacturable structure. The importance of strut thickness derives from the fact that a pattern with dimensions of 20 x 20 mm has cells with dimensions of 4 x 4 mm, considering, for example, five cells per side. Struts thinner than 1 mm would make manufacture more demanding. From a biological point of view, in the perspective of the presence of a transmural infarct, the patch, with realistic thickness equal to 1 mm, must be able to conduct an electric current equivalent to the one that flows through the wall of the ventricle (i.e., 10 mm), but through a thickness that is ten times smaller. To achieve this target, and contemporarily get thicker struts, it was increased the range of constraints for the conductivity of five/ten times. The purpose remains to create as little interference as possible with the heart tissue mechanical behaviour. Considering this, constraints can be adjusted and made more restrictive.
Various conductive materials documented in the literature were examined, leading to the generation of numerous unit cells with properties that fell within the ranges of cardiac tissue ones. For the sake of simplicity, one cell made of PANi and PCL [6] was selected (Figure 1). The bulk material has Young's modulus equal to 2 MPa and conductivity equal to 3.9 S/m.

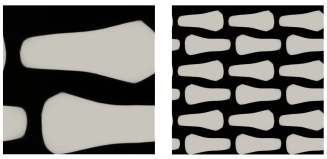

Figure 1: PANi and PCL unit cell and pattern.

The homogeneous properties of the cell are illustrated in Table 1.

Table 1: Properties of cell in Figure 1.

E_1 [MPa]	ν	E_2/E_1	k_1 [S/m]	k_2/k_1
0.62	-0.21	0.31	1.57	0.36

The entire procedure followed in this thesis can be declined for all the other solutions found.

3. Morphological characterisation of the left ventricle from clinical images

In order to simulate the behaviour of the patch, both from a mechanical and conductive point of view, a model of ventricle onto which applying the patch must be generated. The 3D reconstruction of the left ventricle involved the use of a set of CCT images in DICOM format (Digital Imaging and COmmunications in Medicine, *.dicom*). The set included the images of the entire heart in a certain, yet unknown, phase of the cardiac cycle. This set was imported into *3D Slicer* and the images were processed using the segment editor function. First of all, an optimal segmentation threshold needed to be selected. Then, it was necessary to manually remove all the parts that were not coincident with the left ventricle. Two models were generated: one was representative of the ventricular cavity, the other represented the ventricle including all the tissue until its external wall. The segmented models were exported in STL format (i.e., Stereo Lithography, *.stl*), and presented several imperfections and very jagged surfaces. Thus, the files were imported into *Autodesk Meshmixer* (Autodesk, USA), for the post-processing and then they were combined using *HyperMesh* (Altair HyperWorks, USA) to create a solid wall filling the gap between them and incorporating a cavity (Figure 2). The model corresponded to an intermediate

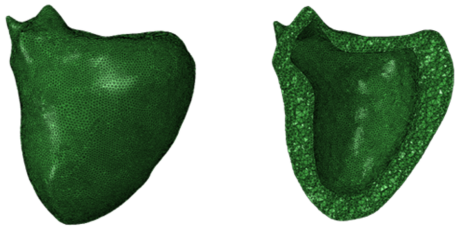

Figure 2: Section of the solid ventricle model.

phase between the end of systole and the end of diastole. Thus, to replicate heart swelling, the model must be scaled to obtain the end-systole configuration. The idea was to derive from the model the volume of the ventricular cavity, and look for volume-related data in literature, in particular considering the phases of end-systole and end-diastole, to select one or more samples such that the measurements of the reconstructed model fell within their range. *Autodesk Meshmixer* allowed to measure the volume of the ventricle model, obtaining an internal cavity volume of 165 ml and a total ventricle volume of 296 ml. The difference between these two values gave the heart tissue volume, i.e., 131 ml, assumed constant during the cardiac cycle. A possible range that finds this values as intermediate was discovered in a study concerning 20 healthy male subjects [4] for whom the volume of the ventricular cavity at end-diastole re-

sulted equal to 181.1 ± 30.3 ml and the volume at end-systole equal to 70.7 ± 18 ml. To scale the cavity model from 165 ml to 70 ml, a *Matlab* code was used, which took as an input a scale factor and the 3D model with *.inp* format and gave as an output the 3D model scaled with the same format. To obtain the model of the external wall of the ventricle in the end-systolic phase, the same procedure was used, knowing that the volume that had to be reached was 70 ml plus 131 ml, since the volume of the tissue was supposed constant. The correct values of volume were approximately reached.

4. Cardiac cycle simulation with pressurization tests

The mechanical computational tests aimed to mimic ventricle filling caused by blood inflow, assessing deformations in the heart tissue and in the patch.

4.1. Tests on parallepiped

To identify the most appropriate material for mimicking cardiac tissue mechanics, initial simulations were performed on a simplified parallelepiped-shaped model that incorporated an infarcted region and a patch. To evaluate the potential advantage of using an auxetic patch, a first simulation was conducted with a solid rectangular-shaped patch, followed by one using the actual patch geometry. The creation of the fully-solid patch in *Abaqus* (Dessault Systèmes, 2019) was straightforward. However, the procedure differed for the auxetic patch as the optimization tool used for its geometry provided a file in *.vtk* format, depicting the material density distribution of the cell. This *.vtk* file had to be imported into *ParaView* (an open source visualization application maintained by Kitware, Inc.) and *3-matic* (Materialise, 2022) for post-processing. For both the infarcted region and the patch a linear elastic material with appropriate properties was imposed. Numerous material models in existing literature describe cardiac tissue mechanics. Fung's model [1] was selected as it has already been implemented in *Abaqus*, through its strain energy function (Equation 1). It demonstrates a transversally isotropic material behavior which differs in the fibre direction (i.e., subscript f) compared to the two orthogonal directions (i.e., subscripts r and s), where the response remains consistent.

$$W = \frac{1}{2} C e^{b_1 e_{ff}^2 + b_2 \left(e_{rr}^2 + e_{ss}^2 + 2 e_{sr} e_{rs}\right)} \cdot \tag{1}$$

$$\cdot\, e^{2 b_3 \left(e_{fs} e_{sf} + e_{fr} e_{rf}\right)} - \frac{1}{2} C$$

The parameters C, b_1, b_2, b_3 were derived experimentally with tests on pig hearts [1]. The incompressibility hypothesis was imposed. The auxeticity of Fung's model is achieved through the arrangement of multiple layers, each with a different fibre orientation. In this particular case, it was decided to partition the model into four layers, following literature [1]. Each layer was associated to a local reference system, aligning direction 1 with a specific fibre orientation (Figure 3). The load applied to the parallelepiped involved a y-direction displacement of 10% of its total length, exerted on the red-highlighted face in Figure 3. Boundary conditions were imposed on the opposite face, including zero y-direction displacement, and one edge of the same face encastred.

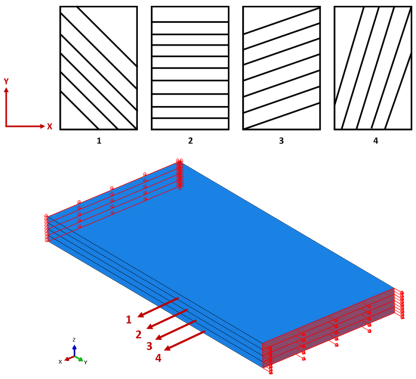

Figure 3: Representation of the partition of the model into the four layers. Schematic representation of the layers and 3D model.

To confirm the auxetic characteristics of Fung's model, the Poisson's ratio of the parallelepiped was calculated, resulting in a value of -0.02. To demonstrate that achieving the same result is not possible without this arrangement of the layers, a mechanical simulation was performed on a model with equally oriented fibres. In this case, the Poisson's ratio value was 0.26. Subsequent simulations incorporated both an infarcted region and a patch, facilitating a comparative analysis of cardiac tissue deformation in four specific scenarios: healthy tissue, tissue with infarction, damaged tissue with a rectangular patch, and damaged tissue with an auxetic patch. The transverse and longitudinal strains of cardiac tissue were acquired for each layer. The results demonstrated the inevitable impact of the infarct due to its higher stiffness. The heart tissue deformations using the auxetic patch were comparable to those in presence of the rectangular patch, but they got closer to those observed in the infarcted ventricle. Moreover, outside the patch region, strain values converged towards cardiac tissue levels. Regarding the most significant deformations in cardiac tissue, the presence of the device was capable of redistributing mechanical overstesses and reduce by approximately 16% the peaks of deformation caused by the infarct, which behaved like a hard inclusion embedded within healthy tissue (Figure 4).

4.2. Tests on semi-ellipsoid

After selecting the Fung's material to replicate heart tissue behavior, the geometry of the model was re-

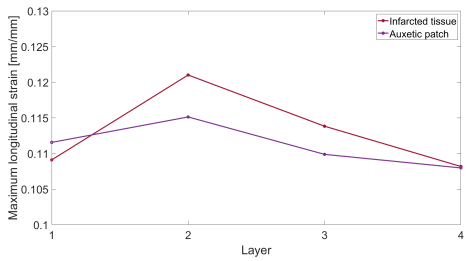

Figure 4: Maximum longitudinal strain for each layer evaluated for infarcted ventricle with and without auxetic patch.

fined to closely resemble that of the left ventricle, maintaining simplicity. Consequently, a hollow semi-ellipsoid was created in *Abaqus* and divided into four layers. Given the model curvature, assigning a local reference system to each layer proved unfeasible. Therefore, a *Matlab* code was developed to systematically divide each layer into 10° wide circular sectors and allocate the pertinent reference system to each of these portions (Figure 5). The imposed load

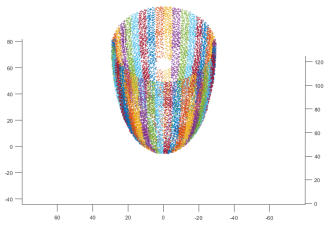

Figure 5: Segmentation of one layer of the healthy tissue into 10° wide portions using *Matlab*.

replicated physiological condition in the left ventricle, with a pressure of 40 mmHg (i.e. 120 minus 80 mmHg) applied to the inner surface of the ellipsoid. Boundary conditions were set by constraining the displacement of the ellipsoid upper portion in all three directions.
Simulations aimed to replicate the volume changes of left ventricle during the cardiac cycle. Despite the considerable variability, an average value for the variation of cavity volume equal to 70 ml was found in literature [4, 5]. In contrast, the volume change experienced by the ellipsoid was 28.7 ml. Thus, modelling the Fung's material with approximations in constructing the layers revealed some limitations, as it didn't accurately predict the expected volume variation. A comparative analysis was conducted to evaluate the strains of cardiac tissue during a simulated heartbeat across three distinct cases: healthy tissue, tissue with infarction, and damaged tissue with the application of an auxetic patch. Longitudinal and circumferential deformations were measured near the patch, confirming results consistent with those of the simplified model. The presence of an infarcted region reduced by approximately 70% the value of deformations in the damaged area. However, this strain variation lowers in the surrounding tissue. Notably, the introduction of the device didn't have a negative impact, as indicated by the similarity in strain trends between infarcted tissue with and without the patch (Figure 6).

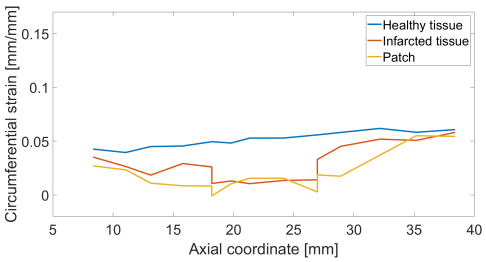

Figure 6: Circumferential strain in axial direction for healthy tissue, infarcted tissue, and damaged tissue with auxetic patch.

4.3. Tests on realistic left ventricle

Although the auxetic material obtained with Fung's model cannot be easily used on complex designs, some simulations were nevertheless performed on realistic ventricle model using a more manageable material. The isotropic Neo-Hookean material was chosen as the simplest hyperelastic alternative approximating the behaviour of the heart, even if it does not truly represent it. This choice was made because its strain energy (Equation 2) is already implemented in *Abaqus* and its coefficients can be derived from well-known properties (i.e. Young's modulus and Poisson's ratio).

$$W = C_{10}\left(\overline{I_1} - 3\right) + \frac{1}{D}\left(J_{el} - 1\right)^2 \qquad (2)$$

C_{10} and D are temperature-dependent material parameters, and $\overline{I_1}$ is the first deviatoric strain invariant. The parameter D was set equal to zero. In this way, *Abaqus* establishes the incompressibility hypothesis. A pressure of 40 mmHg was applied to the inner ventricle wall as for the ellipsoid. Boundary conditions were set by limiting the displacement of both the mitral valve area and the aorta in all three directions.
Before applying the Neo-Hookean material to the complex heart model, a preliminary simulation was conducted on the ellipsoid. The pressurization test yielded a volume change of 50 ml, which is closer to physiological conditions than the result obtained with Fung's model. Considering deformations, data showed distinct behavior between the Neo-Hookean and Fung's materials. One of the reasons is that the former is isotropic, and the latter has auxetic properties. Nevertheless, it was decided to employ the Neo-Hookean material for the heart model to assess vol-

ume changes and deformations. The ventricle experienced a volume change of 46.3 ml, aligning with literature data. Subsequently, longitudinal and circumferential deformations in cardiac tissue were assessed. The healthy ventricle exhibited deformations of approximately 10% in both directions, consistent with existing literature [3]. In presence of an infarcted region, these strains decreased to less than 1%, but they returned to levels comparable to healthy tissue outside the damaged area. In this scenario as well, the patch followed the deformation pattern of the infarcted heart, without having a negative impact on it (Figure 7).

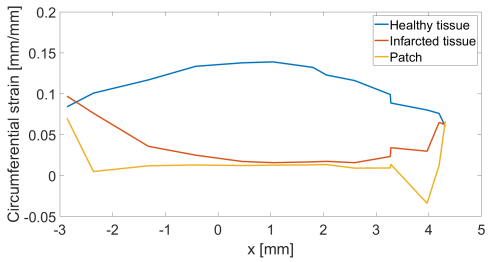

Figure 7: Circumferential strain in x-direction for healthy tissue, infarcted tissue, and damaged tissue with auxetic patch.

5. Simulation of the electrophysiology of the heart

To verify that the designed patch was able to transmit the electrical signals conducted through myocardial cells, an *in silico* model was created. The Ten Tusscher's model was used. It is a mathematical representation of human ventricular cell electrophysiology, that uses key ionic currents to simulate action potential generation. It employs differential equations to describe cell behavior, accounting for stimulus-induced current and transmembrane ionic currents [11].

To simulate the cardiac action potential propagation, *LS-Dyna* (Ansys Inc., 2022) was used. The input to the simulations was a *.k* file, and contained, among others, the following information: the time increment between one calculation step and the following one, the mesh structure of the model, the parts the model was divided into and the material it was assigned to them, the conductivity values of both cardiac tissue and the patch, the parameters of the selected cellular model, the characteristics of the applied stimulus, and the solving method of the problem, i.e., electrophysiology bidomain or monodomain. The former is the most complete model of cardiac electrical activity and it consists of two equations describing intra- and extra-cellular potentials, coupled with a system of equations describing ionic currents. The latter is a simplified model and consists of an equation describing the evolution of the transmembrane potential coupled with an ionic model.

5.1. Simulations on simplified model

The simulations were preliminarly conducted on a simplified model of both heart tissue and patch, to better understand how to set up the parameters for more complex models. Using *LS-PrePost* (Ansys Inc., 2022), the heart was represented with a parallelepiped following a model used in literature [9]. The patch had the same shape and it was positioned at the centre of the upper surface of the heart model and adherent to it (Figure 8). To simulate an infarct, a part was created below the patch and through the entire thickness of the heart tissue model.

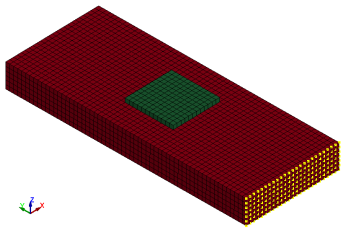

Figure 8: Simplified model of heart tissue and patch. The nodes highlighted in yellow constitute the set from which the stimulus starts.

The conductivity values in direction x, y and z for the healthy heart tissue were set equal to 0.06 S/m, 0.2 S/m and 0.06 S/m, respectively. For the remaining parts, the conductivity had the same value in all directions, corresponding to 0 S/m for the infarct and 3.9 S/m for the patch. The fibers were assumed to be oriented along y-direction. The stimulus corresponded to a healthy heart beat. It started from the nodes of the face shown in Figure 8, had a duration of 2 ms, an amplitude of 50 mV, and a period of 1 second. It followed y-direction, crossing both the infarct and the patch. Given the simplicity of the model, bidomain was chosen due to its greater precision. The outcomes indicated that the patch efficiently conducted the potential transmitted by the heart, in fact, external potential registered on the patch had the same trend of the one on the healthy heart tissue (Figure 9).

5.2. Simulations on heart model

The positive result enabled the transition to a more realistic model (i.e., the one described in section 3). An infarcted region was created in the model, and a simplified parallelepiped-shaped patch conforming to the heart curvature was added above it. To mimic the physiological action potential propagation in the ventricle, stimulation originated from the apex, moved toward the base, and progressed from the endocardium to the epicardium. Accordingly, a set of nodes was established on the inner wall of the apical section. To select the resolution method, two simula-

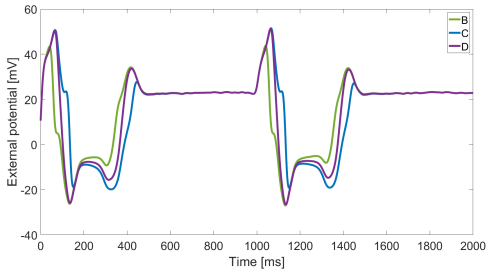

Figure 9: External potential of three nodes of the simplified model: before (B), after (C) and above the patch (D).

tions with identical inputs were conducted, altering only the parameter distinguishing monodomain from bidomain. For simplicity, a physiological heartbeat was simulated using the healthy ventricle model, and differences emerged in the action potential temporal evolution between monodomain and bidomain. Consequently, the bidomain method was favored for its superior accuracy.
A physiological heartbeat was simulated under three conditions: healthy heart tissue, infarcted tissue, and a patch applied to the damaged region. The transmembrane potential was evaluated for healthy heart tissue and infarcted region, constituted by active conductive materials (i.e., they can carry a source). In contrast, the patch, a passive conductive material, lacks a transmembrane potential, so only its external potential was considered. Three nodes on the outer surface of the ventricle were analyzed: one in the infarcted region (i.e., node C), the others in the healthy tissue just before (i.e., node A) and after the patch (i.e., node B). Results (Figure 10) showed that the infarct maintained its transmembrane potential at the resting value of -85.23 mV, thus not propagating the action potential. Considering the three sce-

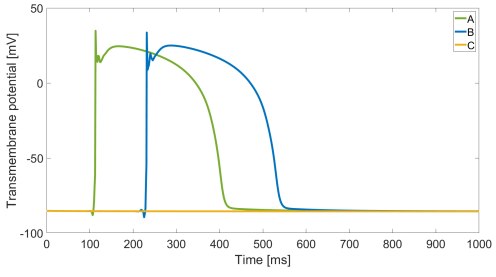

Figure 10: Temporal evolution of action potential in the three selected nodes of the heart.

narios, action potential characteristics for the nodes before and after the patch were derived using a *Matlab* code. These properties include action potential amplitude (APA [mV]), action potential duration at 90% repolarization (APD [ms]), maximum upstroke rate (dV/dt max [mV/ms]), resting membrane potential (RMP [mV]), and maximum potential value (V_{max} [mV]). The simulation results, when comparing the three cases, demonstrated that these characteristics remained consistent for the node after the patch. A delay in activation time of this node was noticed in presence of the infarct, and it reduced its value with the application of the patch. Furthermore, a node on the device was selected to illustrate its conductivity characteristics, and the results demonstrated its ability to track the extracellular potential of the heart tissue.
To test the conductivity of the patch also in an anomalous situation, an extra systole was simulated by creating a second set of nodes from which a stimulus with a duration of 2 ms and an amplitude of 200 mV started. This extra stimulus induced a spiral-shaped action potential, simulating a possible cardiac arrhythmia. This occurs when the action potential encounters cardiac tissue not yet at its resting potential and therefore not responsive. The potential spreads solely through excitable heart tissue and extends to other zones only after they exit the refractory state.
The test was run on healthy heart tissue, a ventricle affected by infarction, and a ventricle with both infarct and patch. The infarcted region remained incapable of conducting the action potential carried by the healthy tissue. Conversely, the patch effectively transmitted the extracellular potential.

5.3. Simulations with auxetic patch

After achieving promising conductivity outcomes, the model underwent further refinement by substituting the simplified patch with the auxetic geometry selected in section 2. Healthy heart tissue was still represented by a parallelepiped. The set of nodes from which the stimulus started and its parameters are the same as those illustrated in Figure 8. To evaluate the conductivity of the patch with its actual geometry, results were estracted similarly to those delineated in subsection 5.1 and subsection 5.2. Figure 11 provides a representation of the extracellular potential at a specific time instant. The results shown in Table 2 demonstrate that the patch effectively conducted the electrical signal without changing the action potential characteristics calculated in two nodes of cardiac tissue, positioned before and after the device.

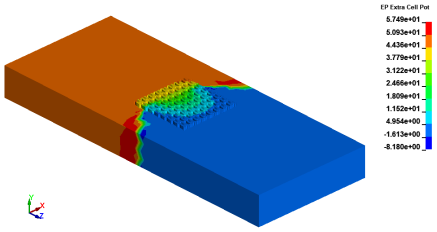

Figure 11: Extracellular potential in a simplified model of the heart with an auxetic patch at instant t = 140 ms.

Table 2: Action potential characteristics for nodes before and after the auxetic patch.

	Node before	Node after
APA	122.21	122.81
APD	296.86	302.30
dV/dt max	346.33	334.85
RMP	-85.23	-85.23
V_{max}	33.36	33.52

6. Conclusions

The investigated patch should substitute the electrical properties lost by the infarcted tissue with minimal alteration to the deformation state established during the cardiac cycle. Therefore, the mechanical properties of the patch should closely resemble those of the heart tissue. The optimization tool used to achieve the patch geometry was well-suited for this purpose. In fact, it requires only a limited knowledge of the bulk material properties, and its outcome demands minimal post-processing to be utilized for a CAD model creation for subsequent analysis. For these reasons, this methodology can extend beyond its current application (e.g., development of medical devices intended to repair various biological structures, including arteries, lung tissue, skin, liver, and more).
The mechanical simulations analyzed how a patch affected ventricular deformation state. The findings suggested that applying a patch to a damaged area did not significantly affect the strain field altered by the infarct. Despite the expected benefits of employing an auxetic patch due to its similarity to heart tissue, simulations on simplified model showed that its performance did not substantially differ from a patch with a positive Poisson's ratio. This outcome may be attributed to the inherent limitations of the conducted tests. The electrophysiological analysis aimed to evaluate the patch conductivity under physiological heartbeat and abnormal conditions, such as extra systole. The findings showed that both auxetic and non-auxetic patches effectively conducted the electrical stimulus in these scenarios while preserving important parameters of the action potential. Consequently, this device stands as a versatile solution when a conductive substrate is required (e.g., cultivation and differentiation of myocardial cells). The main limitation of this study was the selection of the material for heart tissue. Specifically, applying Fung's material to a four-layer model involved a significant approximation, deviating from the anatomical three-dimensional architecture of the myocardium with multiple layers. Moreover, the coefficients associated with this material were experimentally derived from porcine hearts and presented considerable variability across the limited number of samples analyzed. To overcome this problem, cardiac tissue should be modelled using materials that are more representative of its behaviour (e.g., Holzapfel-Ogden model). For a more comprehensive analysis, a multiphysics simulation is required, considering both the mechanical stresses applied on the ventricle and the action potential propagation.
It's worth noting that this study is a preliminary step in the development of a patch with therapeutics properties, thus it doesn't permit a cost-benefit analysis at this point. However, it lays the groundwork for future and more extensive research on the subject.

References

[1] Kevin F. Augenstein et al. Estimation of Cardiac Hyperelastic Material Properties from MRI Tissue Tagging and Diffusion Tensor Imaging.

[2] Parth Chansoria, Emma L. Etter, and Juliane Nguyen. Regenerating dynamic organs using biomimetic patches.

[3] Chansoria et al. Rationally Designed Anisotropic and Auxetic Hydrogel Patches for Adaptation to Dynamic Organs.

[4] Clay et al. Normal Range of Human Left Ventricular Volumes and Mass Using Steady State Free Precession MRI in the Radial Long Axis Orientation.

[5] Nemes et al. Left ventricular apical rotation is associated with mitral annular function in healthy subjects. Results from the three-dimensional speckle-tracking echocardiographic MAGYAR-Healthy Study.

[6] Fábio F. F. Garrudo et al. Electrical stimulation of neural-differentiating iPSCs on novel coaxial electroconductive nanofibers.

[7] Matteo Gavazzoni, Nicola Ferro, Simona Perotto, and Stefano Foletti. Multi-Physics Inverse Homogenization for the Design of Innovative Cellular Materials: Application to Thermo-Elastic Problems.

[8] Michaella Kapnisi et al. Auxetic Cardiac Patches with Tunable Mechanical and Conductive Properties toward Treating Myocardial Infarction.

[9] Steven A. Niederer et al. Verification of cardiac tissue electrophysiology simulators using an N -version benchmark.

[10] Claudio Rugarli and Federico Calogaris Cappio. *Medicina interna sistematica*. Edra : Masson, 7. ed edition.

[11] K. H. W. J. Ten Tusscher and A. V. Panfilov. Alternans and spiral breakup in a human ventricular tissue model.